Computational Analysis of Isothermal Flow in a Test Swirl Combustor

A. C. BENIM
Department of Mechanical and Process Engineering
Duesseldorf University of Applied Sciences
Josef-Gockeln-Str. 9, D-40474 Duesseldorf
GERMANY

M. P. ESCUDIER
Department of Engineering
University of Liverpool
Chadwick Building, Peach Street, Liverpool L69 7ZE
UK

A. NAHAVANDI
Department of Mechanical and Process Engineering
Duesseldorf University of Applied Sciences
Josef-Gockeln-Str. 9, D-40474 Duesseldorf
GERMANY

K. NICKSON
Department of Engineering
University of Liverpool
Brownlow Street, Liverpool L69 3GH
UK

K. J. SYED
Combustor Development
Siemens Industrial Turbomachinery Ltd.
PO Box 1, Waterside South, Lincoln LN5 7FD
UK

Abstract: - Isothermal flow in an idealized swirl combustor is analyzed numerically and experimentally. The Reynolds number based on combustor inlet diameter and mean axial velocity is 4600. Measurements of time-averaged swirl and axial velocity components and corresponding rms turbulence intensities are performed by Laser Doppler Anemometry, along radial traverses at different axial locations. In three-dimensional, transient computations, Large Eddy Simulations (LES) and Unsteady Reynolds Averaged Numerical Simulations (URANS) are employed for modeling the turbulent flows. For LES, the Smagorinsky model is used to model the subgrid scale turbulence. For URANS, the Reynolds Stress Model (RSM) is employed as the statistical turbulence model. The URANS-RSM approach is observed to perform rather poorly. This is assumed to be due to the fact that the present flow has a rather low Reynolds number, and the applied RSM, being a high Reynolds number model, is not able to model low Reynolds number effects. On the other hand, a very good agreement of the LES predictions with the measurements is observed.

Key-Words: - Turbulent Swirling Flows, LES, URANS, RSM, CFD.

1 Introduction

Accurate prediction of the mean flow in a swirl-stabilized gas-turbine combustor still represents a major challenge more than thirty years after Jones and Launder (1972) [1] introduced the k-ε turbulence model. For modeling general turbulent flows, there has been, in the mean time, a move first toward Reynolds stress models (RSM) and algebraic stress models (ASM) and more recently to large eddy simulation (LES), detached eddy simulation (DES) and finally direct numerical simulation (DNS). Even for the isothermal flow with which this paper is concerned, DNS is not yet a practical procedure whereas LES has already been used to compute high Reynolds number combusting flow in a combustor geometry [2]. For turbulent swirling flows, although turbulent viscosity based two-equation models (TVM) such as the k-ε model have continued to be developed and used [3], the majority of recent simulations of intensely swirling flows have been carried out employing ASM [4] and RSM [5,6]. In turbulent viscosity based turbulence models (TVM) a proportionality between the rate of deformation tensor and the Reynolds stress tensor through a scalar turbulent viscosity is presumed. However, in turbulent swirling flows, Reynolds stresses are so strongly influenced by flow curvature and pressure gradient that such a proportionality cannot be justified [7]. This flow structure, where an "isotropic" turbulent viscosity cannot be assumed, will be referred to as "non-isotropic" in the following, and this should not be confused with the isotropy referring to the equality of the diagonal components of the Reynolds stress tensor. This limitation of TVM calls for the application of RSM for turbulent swirling flows, which can principally capture non-isotropic turbulence structures. Thus, as mentioned above, RSM has been widely used in modelling turbulent swirling flows.

However, to the best of the authors' knowledge, the RSM applications in turbulent swirling flows were performed within the framework of conventional, steady-state, RANS formulations (Reynolds Averaged Numerical Simulations). However, as has been demonstrated recently [8], RSM can also lead to serious errors for some highly swirling turbulent flows, when applied within the framework of RANS. The reason seems to be that the low frequency transient motion of coherent structures, which can play an important role in turbulent swirling flows, cannot adequately be represented by RSM (or by any other statistical turbulence model).

Therefore, the use of RSM within the framework of a URANS (Unsteady RANS) formulation has recently been proposed [9,10]. Since the above-mentioned flow transience is closely related with three-dimensionality, the transient URANS-RSM formulation needs to be applied within the framework of a three-dimensional formulation, even if the flow geometry and boundary conditions are axisymmetric and in steady-state (apart form turbulent fluctuations). LES has also been identified [9,10] as potentially capable of accurately predicting turbulent swirling flows, as the non-isotropic turbulence structures are known to be dominant in the large scales, which are resolved by LES.

The present paper can be seen as a continuation of the previous validation study [9,10], where the flow in the experimental water test rig of Escudier and Keller [11] was investigated. For the present flow, the Reynolds number is 4600, whereas this was about 7000 in the previous study [9,10]. Thus, the present flow is more demanding, as far as the low Reynolds number (low-Re) effects are concerned. In the present study, URANS-RSM and LES models are used as turbulence models.

2 Experimental

Experiments were performed for water flow through the model combustor sketched in Fig. 1. The swirl generator (Fig. 2) is based upon the tangential-inlet design of Escudier et al (1980) [12]. However, instead of a single wide slit [12], 12 narrow slits at 30^o intervals are used in the present design. Slits were generated using 12 identical wedges assembled around a vertical axis. The wedges are produced from stainless steel and the width of each slit is 1 mm. The outer diameter of the wedge assembly is 165 mm and the inner channel created by the wedges is a dodecahedron with distance between opposing flat surfaces 55 mm. The open axial length of the slits L_S can be changed between 27 and 263 mm by adjusting the axial position of a close-fitting central piston. The swirl generator is surrounded by a cylindrical jacket of inner diameter 305 mm into which water is fed through six equally spaced 31 mm diameter inlet ports each angled to be tangential to the periphery of the wedge assembly and located half way along its length. The water is fed under gravity from a tank some 36 m above the vortex generator, the flow rate being controlled by two needle valves arranged in parallel.

As shown in Fig. 1, the combustor inlet diameter D_I is 50 mm and the inlet is located 65 mm downstream of the exit of the swirl generator. The body of the combustor itself has an initial diameter D_C of 100.4 mm which after a length of 170 mm tapers over a distance of 125 mm to an outlet diameter D_E of 40 mm. The entire model is vertical with a bulk upward flow discharging from the outlet tube into a large collection tank. In the latter, the water level is below that of the outlet tube. Thus, a free surface is formed at the outlet.

Radial distributions of the time-averaged axial (u) and swirl (w) velocity components, and the corresponding rms turbulence intensities (u' and w') were measured in forward-scatter using a Dantec Fibreflow laser Doppler anemometer (LDA) system comprising a 60X10 probe

and 57X08 receiving optics. The beam separation at the front lens was 51.5 mm and the lens focal length 160 mm

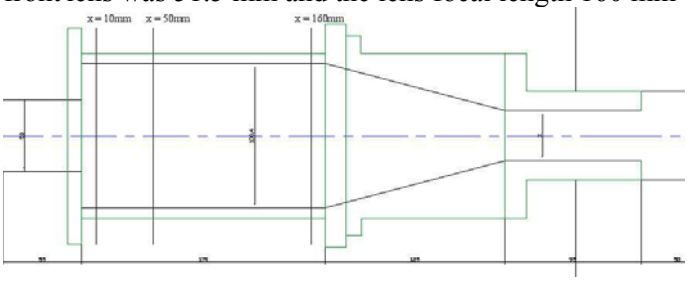

Fig. 1. Schematic of test combustor
(model vertical, bulk flow upwards)

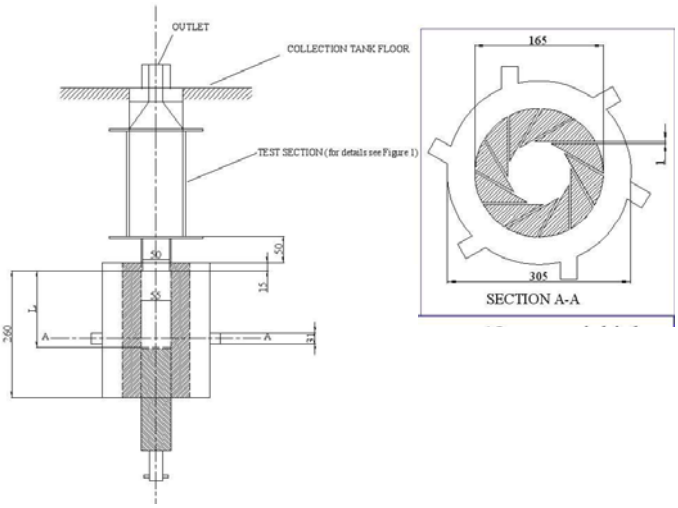

Fig. 2. Schematic diagram of swirl generator.

which produced a measuring volume 280 μm in length and 45μm in diameter. The measurement locations, indicated in Fig. 1 were x = 10mm, 50mm and 160 mm, where the axial distance x is measured from the inlet to the combustor. The Reynolds number based on the mean axial velocity at the combustor inlet and the combustor inlet diameter was 4600.

3 Modeling

The analysis is based on the general-purpose CFD code ANSYS-CFX [13], which is a vertex-centered finite volume method and treats the continuity and Navier-Stokes equations by a coupled solver in conjunction with an unstaggered, unstructured grid definition.

In the main computations, i. e. in computing the flow in the combustor section, transient, three-dimensional strategies such as URANS) and LES are employed for treating turbulence. However, for computing the low-Re flow through swirl generator slits, for obtaining inlet boundary conditions for combustor domain, the low-Re k-ε model of Launder and Sharma [14] is used. Within the framework of URANS, the Reynolds Stress Model (RSM) of Speziale, Sarkar and Gatski [15] is employed, using a quadratic approximation for the pressure-strain correlation. This approach was recently demonstrated [16] to be superior to the alternative formulation by Launder, Reece and Rodi [17] which applies a linear correlation. The employed RSM is a high-Re one, amended by the wall-functions approach for the near-wall flow [18].

In LES [18], the Smagorinsky model [19] is used as the subgrid scale model, with a constant model coefficient of C_S=0.1. The subgrid-scale viscosity is explicitly brought to zero in the vicinity of solid boundaries by the Van Driest damping function [20].

The water test rig has a vertical orientation with upward flow direction. The water leaving the duct exits the test section by spilling out radially into a chamber, forming a free surface with the ambient air, located a few millimetres above the wall. This outlet geometry is modelled as realistically as possible, by letting the solution domain to extend up to this free surface, and assigning a zero-shear, slip boundary condition at this boundary. The rather tiny circumferential ring area remaining between the outer edges of the rig wall and the modelled free surface is defined to be the outlet boundary, assigning zero-gradient boundary conditions.

For URANS-RSM, the advection terms of the momentum equations are discretized by a high resolution scheme [22]. For the advection terms of the transport equations of the Reynolds stresses and dissipation rate of the turbulence kinetic energy, an upwind difference scheme [23] is applied. In LES, the central differencing scheme [23] is used to discretize the advection terms of the momentum equations. For the transient term, a second order backward Euler scheme [23] is used.

4 Results

The swirl generator has a dodecahedron cross-section, with distance between opposing surfaces 55 mm. The combustor has a circular inlet with a slightly smaller diameter of 50 mm. The "imaginary" cylindrical surface, created by an "extrusion" of the circular combustor inlet along the swirl generator axis is defined to be the inlet boundary of the combustor domain. For determining the combustor inlet boundary conditions, RANS computations are performed for a solution domain covering the plenum, the slits and the swirl generator. Utilizing the periodicity of the flow, three-dimensional computations have been performed for a wedge-shaped domain covering a single slit, i.e. the $1/12^{th}$ of the whole circumference. The block-structured grid consisted of approx. 500,000 hexahedral cells. For modeling the very low Reynolds number flow in the slits, the low-Re number k-ε model [14] is used. Special care is paid for a sufficiently fine resolution of near-wall regions,

fulfilling the condition of $y^+<1$ for the near-wall cells. The results are used as inlet boundary conditions for the main simulations of the combustor flow.

For the main computations, i. e. for the computations of the combustor flow, a three-dimensional conformal block-structured consisting of 1,000,000 hexahedral finite volumes is generated. based on the previous 2D grid. A three-dimensional grid independency study has not been performed. The 3D employed here grid is based on a preliminary grid independency study performed for a 2D-axisymmetric, steady-state analysis.

The surface grid is shown in Fig. 3a in perspective view. A longitudinal section of the 3D grid is shown in Figure 3b in detail view. As seen in the figure, the aspect ratios of the cells are very close to unity especially in the inlet section of the combustor, where the vortex breakdown is expected. In generating the 3D grid, based on the 2D grid, the number of cells in the circumferential direction is adjusted in such a way that the ratio of the circumferential cell width to the radial cell width was close to unity in the central regions and remained moderate on the combustor wall (aspect ratio below 5). A cross-section of the 3D grid in the combustor is shown in Figure 3c.

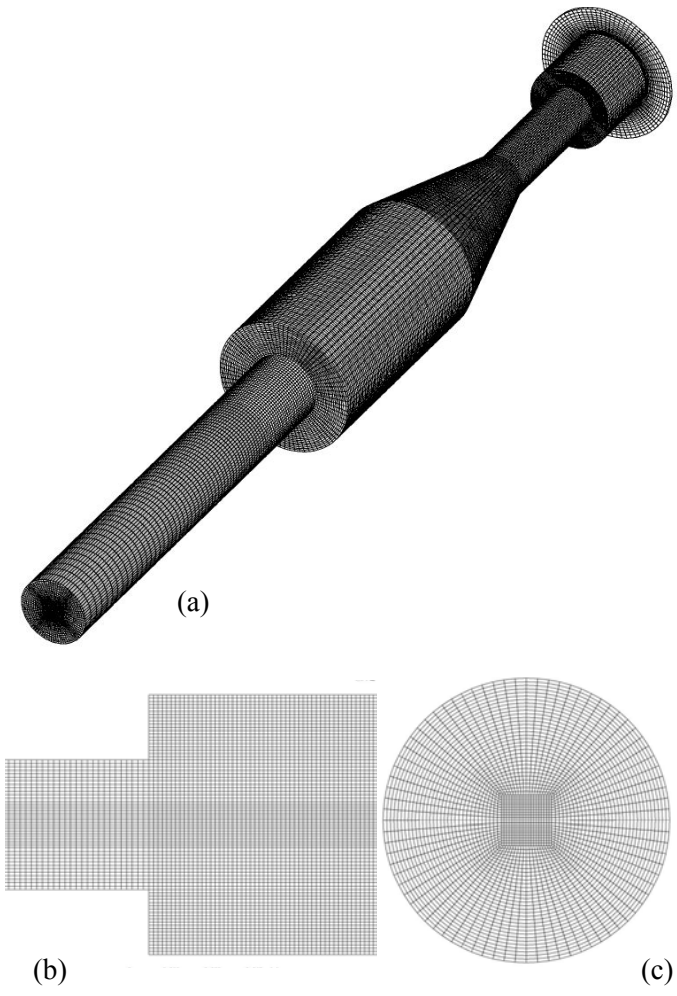

Fig. 3. Computational grid; a): surface grid, b): longitudinal section (detail), c): cross-section.

The resulting y^+ values with the present grid are quite optimal ($y^+\approx30$) for the application of the wall-functions approach. In URANS-RSM and LES computations, both, the same grid, and the wall-functions approach is used near the walls. Generally speaking, the wall-functions approach would not be suitable for LES. Nevertheless, we assume that this inaccuracy will not cause a serious inaccuracy in LES predictions, since the main flow features such as the internal recirculation zone are of the "free shear layer" type rather than "wall driven".

Turbulent viscosity based turbulence models used initially for 3D URANS could not capture any flow transience, but converged to a steady-state axisymmetric flow field. Such results of the $k-\varepsilon$ model have been used as initial conditions for the present computations. Having started the URANS – RSM and LES computations from this initial solution, computations are carried out for a period of time, which is long enough to allow the flow transience to develop fully. This is judged by monitoring flow variables at selected points. This state is normally achieved within about 3s flow time. Thereafter, the time averaging of the results has been started. Time averaging is carried out until the average solution no longer shows substantial changes in time. Ideally, the time averaging should be performed until perfectly smooth and, in our case, perfectly axissymmetrical time-averaged distributions are obtained. Nevertheless, it has been observed that it takes an extremely long time to achieve a perfect smoothness (except for URANS-RSM computations). Therefore, when we could conclude that the main time-averaged flow structure would show no further substantial changes (other than a rather small scale smoothing), the computations were stopped. For this reason, the time-averaged results presented here exhibit some small asymmetries and oscillatory behaviour, which are, but, believed not to be detrimental for the main conclusions to be drawn.

The computations are carried out using a time step size of $2.5\cdot10^{-4}$ for both models. The resulting maximum cell Courant numbers [23] remained below 0.8. The time step size is also compared with the resulting Kolmogorov time scales [20]. It has been observed that the ratio of the time step size to the local Kolmogorov time scale always remained around unity. Thus, for the present computations, it can be assumed that the temporal resolution was sufficiently accurate. For the LES computations, the ratio of the local filter width (grid size) to the local Kolmogorov length scale [20] was about 7 on the average. The local maximum value of this ratio was about 12. Recently it was shown [24] that this ratio should be less than 10 to obtain a DNS-like accuracy in LES computations. Thus, the present values indicate that the spatial resolution is quite ideal, and a good accuracy should be expected.

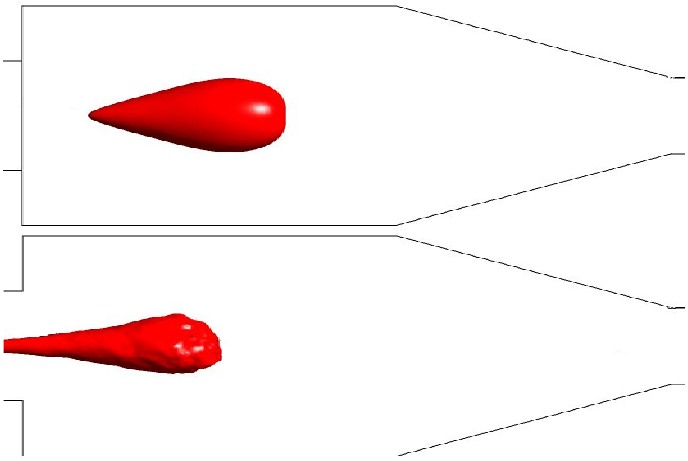

Fig. 4. Time-averaged iso-surfaces of zero axial velocity predicted by URANS-RSM (above) and LES (below).

Time-averaged shapes of the zero axial velocity iso-surfaces predicted by URANS-RSM and LES are presented in Fig.4. The smoother time-averaged iso-surface obtained by URANS-RSM implies that transient, three-dimensional structures captured by URANS-RSM are of larger scale, compared to the turbulent motion of large eddies captured by LES. URANS-RSM predicts a closed bubble in the combustor, whereas the recirculation zone predicted by LES extends deep upstream into the swirl generator.

Predicted and measured radial profiles of time-averaged axial (u) and swirl (w) velocities as well as rms fluctuations of axial (u') and swirl (w') velocities at the axial position x=10mm are shown in Fig. 5 (the velocities and the radial coordinate are non-dimensionalized by average axial inlet velocity U_I, and combustor radius R, respectively). For u (Fig. 5a), the experimental data shows reverse flow both on the axis as well as in the corner downstream of the sudden expansion into the combustor. The mean flow characteristics are captured exceptionally well by the LES, while the URANS RSM (indicated as "U RSM" in the figure) performs rather poorly producing a slight velocity deficit on the centreline but no flow reversal. For w (Fig. 5b), the LES calculations agree very well with the data. URANS RSM underpredicts the peak values remarkably. For u' (Fig. 5c), the URANS RSM calculation picks up little of the fine detail and is clearly unsatisfactory whereas the LES calculations are generally in a quite good agreement with the measurements, the greatest discrepancy being at the radial location where u is a maximum ($r \approx 0.4R$). For w' (Fig. 5d), the performance of both models is comparably less satisfactory in the outer recirculating flow ($r>0.5R$) where w is relatively uniform. Again LES performs still better than URANS-RSM. For u' and w', the peaks at $r \approx 0.5R$ are well reproduced by the LES calculations and just evident in the URANS RSM calculation.

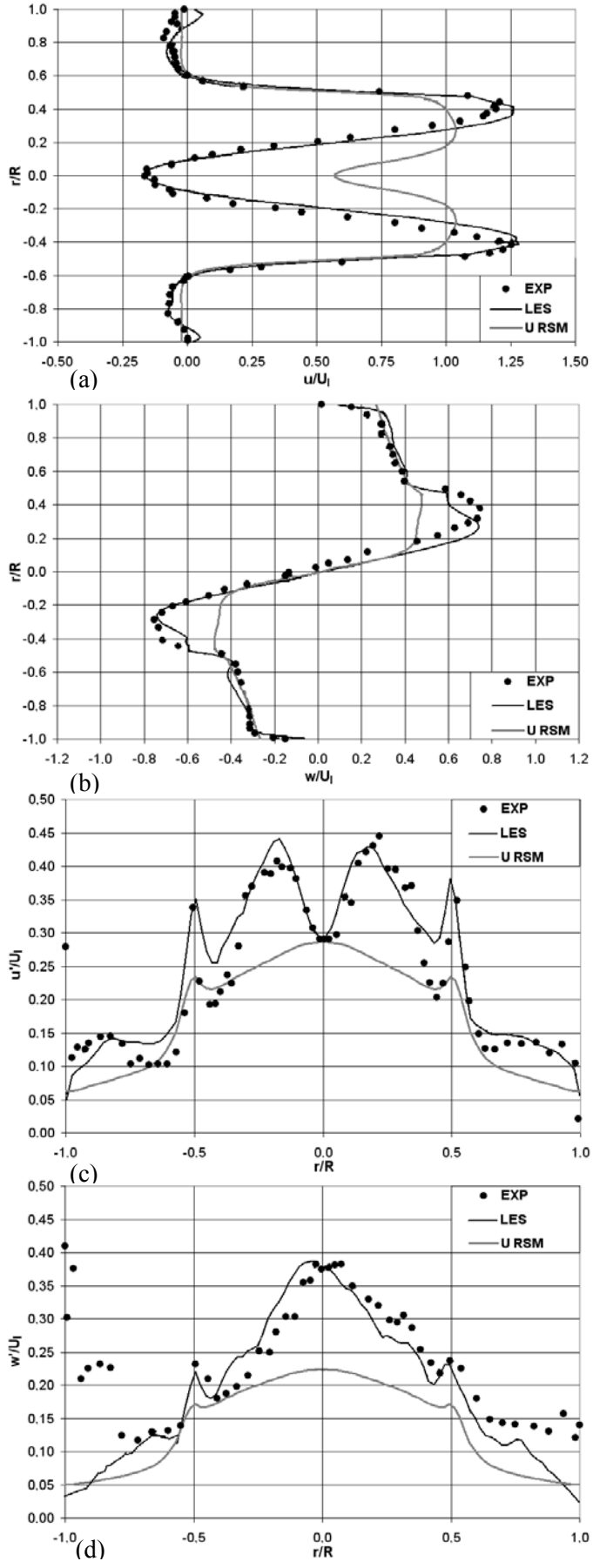

Fig. 5. Experimental and predicted profiles at x=10mm, (a) mean axial velocity (b) mean swirl velocity, (c) rms fluc. of axial velocity, (b) rms fluc. of swirl velocity

5 Conclusions

Isothermal water flow in an idealized swirl combustor operating at Reynolds number 4600 is investigated numerically and experimentally. Measurements of time averaged velocity components and corresponding rms velocity fluctuations are performed by LDA along traverses at different axial locations. In transient, three-dimensional computations, URANS RSM and LES strategies are employed to model the turbulent flow. A very good agreement of the LES predictions with the experiments is observed. The performance of URANS RSM was rather poor compared to LES. A reason for this is assumed to be that the present flow has a rather low Reynolds number, and the applied RSM, being a high Reynolds number model, is not able to model low Reynolds number effects, whereas LES seems to cope better with this situation. Further comparisons between predictions and experiments under different operating conditions will be discussed in the oral presentation.

References:

[1] Jones, W. P. and Launder, B. E., "The prediction of laminarisation with a two-equation model of turbulence", International Journal of Heat and Mass Transfer, Vol. 15, 1972, pp. 301-314.

[2] Moin, P, "Large eddy simulations of multi-phase turbulent flow in realistic combustors", Progress in Computational Fluid Dynamics, Vol. 4, 2004, pp. 237-240.

[3] Xia, J. L., Smith, B. L., Benim, A. C., Schmidli, J. and Yadigaroglu, G., "Effect of inlet and outlet boundary conditions on swirling flows", Computers & Fluids, Vol. 26, 1997, pp. 811-823.

[4] Weber, R., Visser, B. M. and Boysan, F., "Assessment of turbulence modelling for engineering prediction of swirling vortices in the near burner zone", International Journal of Heat and Fluid Flow, Vol. 11, 1990, pp. 225-235.

[5] Hogg, S. and Leschziner, M. A., "Computation of highly swirling confined flow with a Reynolds stress turbulence model", AIAA Journal, Vol. 27, 1989, pp. 57-63.

[6] Jakirlic, S., Jester-Zürker, R. and Tropea, C., "Joint effects of geometry confinement and swirling inflow on turbulent mixing in model combustors: a second moment closure study", Progress in Computational Fluid Dynamics, Vol. 4, 2004, pp. 198-207.

[7] Sloan, D. G., Smith, P. J. and Smoot, L. D., "Modelling of swirl in turbulent flow systems", Progress in Energy and Combustion Science, Vol. 12, 1986, pp. 163-250.

[8] Benim, A. C. and Nahavandi, A. "A computational analysis of turbulent swirling flows", in Hanjalic, K., Nagano, Y. and Tummers, M. J. (Eds.), Turbulence, Heat and Mass Transfer 4 (Begell House, New York, 2003) pp. 715-722 .

[9] Benim, A. C., Nahavandi, A. and Syed, K. J., "URANS and LES analysis of turbulent swirling flows", Progress in Computational Fluid Dynamics, Vol. 5, 2005, pp. 444-454.

[10] Benim, A. C., Nahavandi, A., Stopford, P. J. and Syed K. J., "DES LES and URANS investigation of turbulent swirling flows in gas turbine combustors", WSEAS Transactions on Fluid Mechanics,Vol.1, 2006, pp. 465-472.

[11] Escudier, M. P. and Keller, J. J., "Recirculation in swirling flows: a manifestation of vortex break-down", AIAA Journal, Vol. 23, 1985, pp. 111-116.

[12] Escudier, M. P., Bornstein, J. and Zehnder, N., "Observations and LDA measurements of confined turbulent vortex flow", Journal of Fluid Mechanics, Vol. 98, 1980, pp. 490-463.

[13] ANSYS-CFX-10 Solver Manual, ANSYS Europe, Oxfordshire, UK, 2006.

[14] Launder, B. E. and B T Sharma, "Application of the energy dissipation model of turbulence to the calculation of flow near a spinning disc", Letters in Heat and Mass Transfer, Vol. 1, 1974, pp. 131-138.

[15] Speziale, C. G., Sarkar, S. and Gatski, T. B., "Modelling the pressure strain correlation of turbulence", J. Fluid Mech., Vol. 227, 1991, pp. 245-272.

[16] Grotjans, H., Menter, F. R., Burr, R. C. and Gluck, M., "Higher order turbulence modeling in industrial applications", Proceedings of the 4th Symposium on Engineering Turbulence Modelling and Measurement", 1999.

[17] Launder, B. E., Reece, G. J. and Rodi, W., "Progress in the development of a Reynolds-stress turbulence closure", Journal of Fluid Mechanics, Vol. 68, 1975, pp. 537-566.

[18] Launder, B. E. and Spalding, D. B., "The numerical computation of turbulent flows", Computer Methods in Applied Mechanics and Engineering, Vol. 3, 1974, pp. 269-289.

[19] Sagaut, P., Large Eddy Simulation for Incompressible Flows – An Introduction, 2nd Ed., (Springer, Berlin, 2002)

[20] Smagorinsky, J., "General circulation experiments with the primitive equations. I: the basic experiment", Month. Weath. Rev., 1963, pp. 99-164.

[21] Hinze, J. O., Turbulence (McGraw-Hill, New-York, 1959).

[22] Barth, T. J. and Jespersen, D. C., "The design and application of upwind schemes on unstructured meshes", AIAA Paper No. 89-0366, 1989.

[23] Peyret, R. (Ed.) Handbook of Computational Fluid Dynamics (Academic Press, San Diego, 2000).

[24] Fröhlich, J., Mellen. C. P., Rodi, W., Temmerman, L. and Leschziner, M. A., "Highly resolved large-eddy simulation of separated flow in a channel with streamwise periodic constrictions", Journal of Fluid Mechanics, Vol. 526, 2005, pp. 19-66.